CEA comité español de automática

XLIV Jornadas de Automática 2023

XLIV Jornadas de AUTOMÁTICA 2023 — ZARAGOZA
https://jautomatica.es

Online 3D LIDAR-based mapping for long-range powerline inspection using UAVs

Rodríguez, I.G., Luna-Santamaría, J., Paneque, J.L., Martínez-de Dios, J.R.*, Ollero, A.

GRVC Robotics Lab, ETSI, Avda. de los Descubrimientos, sn, 41092, Sevilla, España.

To cite this article: Gutiérrez-Rodríguez, I., Luna-Santamaría, J., Paneque, J.L., Martínez-de Dios, J.R., Ollero, A. 2023. Online 3D LIDAR-based mapping lor long-range powerline inspection using UAVs. XLIV Jornadas de Automática 599-604. https://doi.org/10.17979/spudc.9788497498609.599

Resumen

Existe una creciente demanda industrial de Sistemas Aéreos No Tripulados (UAVs) autońomos para la inspección de infraestructuras eléctricas. Actualmente el mapeo de las líneas eléctricas se realiza en dos etapas: 1) recolección de datos mediante vehículos aéreos tripulados o no tripulados equipados con LiDAR, cámaras y otros sensores; 2) procesamiento a posteriori de los datos de vuelta en el laboratorio. Este procedimiento es ineficiente y en muchas ocasiones requiere la repetición de los vuelos tras varias semanas para volver a tomar datos. En este artículo se presenta un sistema robótico completamente autónomo para la obtención en tiempo real de mapas 3D basados en LiDAR en misiones de inspección de largo alcance de líneas eléctricas. El sistema propuesto ha sido validado en misiones BVLS con vuelos fuera de la línea de vista (> 3.5 km) en diferentes escenarios de infraestructuras eléctricas con distintas condiciones del entorno y de vegetación. Este artículo presenta el problema planteado, los métodos de mapeo empleados, el diseño del robot, los experimentos realizados y algunos resultados obtenidos.

Palabras clave: Robots aéreos, Sistemas robóticos autónomos, Percepción para robots.

Online 3D LIDAR-based mapping for long-range powerline inspection using UAVs

Abstract

There is a strong industrial demand to develop autonomous Unmanned Aerial Systems (UAVs) for long-range inspection of the electric system. Powerline mapping is currently performed in two stages: 1) data collection by manned or unmanned aerial vehicles equipped with LiDARs, cameras, and other sensors, and 2) offline data processing in the laboratory. This procedure is inefficient and frequently requires to repeat the data collection flights after a number of weeks. This paper describes an aerial robotic system for online and on board building LiDAR-based maps for long-range powerline inspection. It includes autonomous navigation and robust online LiDAR-based mapping methods also integrating GNSS. The system has been validated in Beyond Visual Line of Sight (BVLS) missions (> 3.5 km) in different powerline scenarios with different types conditions and vegetation. The paper describes the problem addressed, the mapping methods used, the designed robot, the experiments, and some obtained results.

Keywords: Flying robots, Autonomous robotics systems, Perception and sensing.

1. Introduction

By regulation, the electric power system should be submitted to periodic inspections, which include detection of defects, measuring distances between the powerline and vegetation, and inspecting electrical towers, insulators, among others. These inspection tasks have been traditionally performed by teams of workers climbing, by means of cranes or man-fits to access the electric assets and powerlines, involving extensive manpower in highly dangerous environments. Powerline inspection has also been performed using manned helicopters that register measurements and images from high accuracy LiDARs and cameras. The collected images and data are post-processed offline (days after data collection) to actually perform the inspection. Besides, using manned helicopters also involves very high costs.

*Autor para correspondencia: J. Ramiro Martínez-de Dios (jdedios@us.es)

The need for cost-effective solutions has motivated intense activity in robots for powerline inspection. Works (Wang et al., 2009) and (Li et al., 2013) describe unmanned autonomous helicopters for powerline inspection using visual and infrared cameras, whereas works (Jwa et al., 2009) and (Zhang et al., 2016) are based on LiDARs. Helicopters are energetically inefficient, which severely constrains their flight endurance. The high energy efficiency of fixed-wing vehicles has motivated their use for long-range powerline inspection. Different commercial products and services have been developed, see e.g., (Yi et al., 2017). Some works, e.g., (Deng et al., 2014), combine the high flight endurance of fixed-wing vehicles with the hovering capacity of multicopters in a multi-platform system. Vertical Take-Off and Landing (VTOL) have also attracted high interest (Wang, 2021; Bhola et al., 2018). VTOLs are capable of hovering in rotary-wing flight mode (enabling high-accuracy inspection of towers or transformers) and also can operate in fixed-wing flight mode (suitable for powerline inspection). Besides, they can take-off and land vertically preventing the need for runways and other infrastructures. The VTOL transitions between fixed-wing and rotary-wing flight require advanced control methods. Also, most existing VTOLs still have significant payload constraints that hamper the onboard installation of suitable LiDARs, cameras, and computers for online processing.

A good number of photogrammetry methods have been developed. Those that can obtain satisfactory accuracy for powerline inspection requirements include complex optimization stages that prevent online execution. Besides, photogrammetry methods have to cope with distortions caused by the potentially strong changes in lighting conditions (i.e., shade/sun).

This work deals with the use of multicopters for the inspection of the electric system. Multicopters have high maneuverability and can hover, being ideal for detailed inspection tasks (Paneque et al., 2019; Perez-Grau et al., 2021), and can also have sufficient payload capacity for installing on board sensors and processing hardware. Further, recent research focus on providing multicopters with the capacity of perching on powerlines for recharging batteries, see e.g., (Kitchen et al., 2020; Paneque et al., 2022), which is interesting to extend their flight endurance. The use of multicopters for powerline inspection has been proposed in commercial systems such as ABJ powerline corridor inspection, and also in scientific works (Liu et al., 2019, 2009). Work (Takaya et al., 2019) collects data and images from an onboard LiDAR and visual camera and process them offline after the flight. Work (Bian et al., 2018) autonomously segments powerlines from images and uses them to guide the robot. In all these systems the inspection process is performed in two stages. First, the multicopter flies through teleoperation or using predetermined missions to register measurements without performing any online processing. Second, in the office/lab, inspection is performed by offline analyzing the collected data using processing and artificial intelligence algorithms (Martinez et al., 2018; Jenssen et al., 2019). In this procedure the operators cannot be sure that the obtained maps have sufficient resolution or accuracy, potentially requiring repeating the data collection flights weeks after the data collection flights, hence involving delays, costs, and operational problems.

This paper presents a fully autonomous robot for online building accurate 3D maps suitable for long-range powerline inspection. It has been developed within the H2020 AERIAL-CORE project (`https://aerial-core.eu/`), which researches in cognitive functionalities for aerial robots and validates them in powerline inspection and maintenance. The proposed system builds online and fully onboard an accurate 3D map of the area surrounding powerlines enabling measuring distances between vegetation and the electrical system. The LiDAR scans are online used for map building and are also processed to detect objects of interest in powerline inspection, providing a semantic 3D map. The robot includes a fully onboard architecture that enables autonomous navigation as well as teleoperation using high-levels commands. The proposed system has been validated in experiments conducted in different powerline environments with different types conditions.

This paper is organized as follows. The general description of the presented system is summarized in Section 2. The LiDAR-based mapping method is sketched in Section 3. The adopted LiDAR segmentation method is presented in Section 4. Section 5 presents the experimental validation. Section 6 concludes the paper and highlights main future research lines.

2. Long-range powerline inspection

Powerline inspection requires measuring the distances between the vegetation, powerlines and towers using a 3D map of the surroundings of the powerlines. The intended aerial robotic system should automatize powerline inspection in long-range missions. It should be able to online build accurate 3D maps using measurements from LiDAR and other sensors. The robot should be endowed with autonomous navigation functionalities; should be able to perform long-range flights; and should allow the possibility of being used in multi-robot schemes.

The proposed system is based on a fully autonomous multicopter aerial robot capable of performing Beyond Visual Line of Sight (BVLS) flights. The robot flies 10 m above the powerline and towers and follows the powerline describing a trajectory specified as a set of waypoints defined by the operator based on existing maps of the electric system. Figure 1 shows the scheme of the adopted architecture. It includes a *Motion planning* module based on Vehicle Routing Problem ((Zhen et al., 2019)) to enable cooperative powerline inspection using several aerial robots. A GNSS-based *Trajectory tracker* module gives the commands to the robot autopilot using UAV Abstraction Layer (UAL) ((Real et al., 2020)). UAL is a middleware created by the GRVC Robotics Lab to simplify the development and testing of aerial robotics methods by standardizing the interfaces with the robots. During navigation, the point clouds from the 3D LiDAR are collected and logged and also processed by module *LiDAR-based mapping* to online build an accurate 3D map of the environment. The robotic system is also endowed with methods that process the obtained LiDAR-based geometrical map to segment the map points into four classes *Powerline*, *Tower*, *Vegetation*, and *Cloud*. The robotic system also includes a *Ground control station* for monitoring the mission and providing high-level commands to the robot.

The method was implemented on the *LR-M* aerial robot developed by the GRVC Robotics Lab from the University of Seville, see Fig. 2. *LR-M* uses the Matrice 600 hexacopter platform from DJI. Its main sensors are a Livox Horizon 3D solid

state LiDAR pointing at a pitch angle of -40 degrees and an Intel RealSense RGB camera mounted with the same orientation for user visualization. Additionally, *LR-M* is equipped with a Jetson NVIDIA NX Xavier for online computation and logging, a DJI GPS receiver, and a Ubiquity radio link for communications. The total weight of the platform was 15.6 Kg. The Livox Horizon is a high-performance solid-state 3D LiDAR that uses lasers at wavelength of 905 nm. It has a field of view of 81.7º × 25.1º, a detection range of 260 m, an angular precision of 0.05°, and a point rate of 240,000 pts/s. It has non-repetitive horizontal scanning pattern, which in contrary to classical fixed-pattern scanning from traditional LiDARs, enables increasing the scanning density even in cases where the multicopter is in hovering mode. The LiDAR is configured in dual-return mode, such that it provides the first and latest return in each measurement, allowing to collect data from beneath the vegetation canopies.

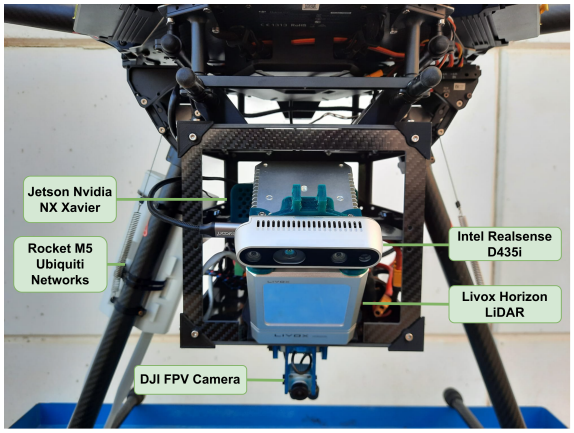

Figure 2: *LR-M* aerial robot developed by the GRVC Robotics Lab using in long-range LiDAR-based mapping highlighting some of its main components.

3. Robust LiDAR-based mapping

This module online builds a 3D map of the area inspected by the robot. The main sensors used are the onboard 3D LiDAR and IMU, and also GNSS to improve accuracy. The built map should have sufficient accuracy to perform geometric and visual inspections with it. The mapping method should be robust to scenarios with low density of geometrical features; should have moderate computational cost to enable its online onboard execution; and should have low memory usage to enable mapping of large-scale scenarios in long-range missions.

The LiDAR-based mapping engine is the main component of this module. A good number of 3D LiDAR-based mapping methods have been developed in the last years. Relevant, recent examples include *LOAM-Livox* (Lin and Zhang, 2020), *Livox-Mapping* (SDK, 2020), *LiLi-OM* (Li et al., 2021) and *FAST-LIO2* (Xu et al., 2022)). All these algorithms operate well in scenarios with high content of geometrical information. However, robustness to scenarios with lack of features is a critical requirement since the robot might traverse very different types of scenarios (and with diverse types of vegetation) during the long-range missions. We performed preliminary experiments in Alcala de Guadaira (Sevilla), in which the robot mapped crops with low vegetation densities (which translated in low densities of features). Figure 3 shows the estimation of the aerial robot location computed by the above algorithms versus the (rotation and translation aligned) ground truth robot location measured with GPS. *FAST-LIO2* provided the highest robustness and accuracy, and thus was selected as the mapping engine in our system.

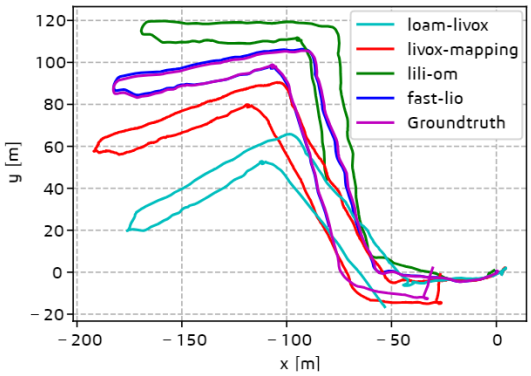

Figure 3: Multicopter location computed by *LOAM-Livox* (Lin and Zhang, 2020), *Livox-Mapping* (SDK, 2020), *LiLi-OM* (Li et al., 2021) and *FAST-LIO2* (Xu et al., 2022)) versus the ground truth robot location measured with GPS (in purple). The trajectories were aligned with the ground truth during the first minute of the flight.

FAST-LIO2 uses efficient data structures such as incremental KD-trees to be able to work directly with full LiDAR scans instead of with feature points as the other methods. Besides, it is based on error-state manifold-based iterative Kalman Filter (*ikFoM*) state estimation in contrast to the optimization-based methods used in the other works. Moreover, it has low memory and CPU consumption and can run online without discarding data, resulting in finer pose estimates than the other methods.

To increase mapping accuracy, *FAST-LIO2* was modified to integrate GNSS measurements in the Update of its iterated Kalman Filter scheme. The measurement model is obtained as

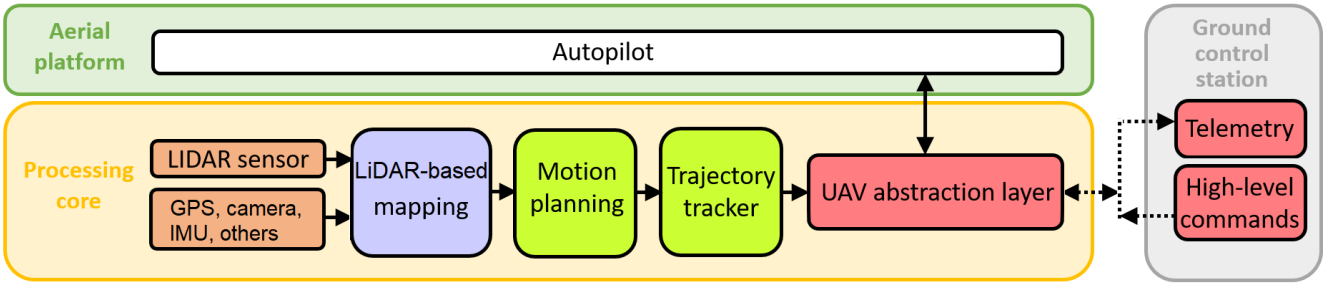

Figure 1: Scheme of the functional architecture of *LR-M* aerial robot.

the current position of the GNSS sensor given the robot state:

$$\mathrm{h}(\mathbf{x}, \boldsymbol{\nu}) = \mathbf{R}_G^W \left(\mathbf{R}_W^I (\mathbf{p}_I + \boldsymbol{\nu}_I) + \mathbf{t}_W^I \right) + \mathbf{t}_G^W, \quad (1)$$

where $\mathbf{x}$ is the state of the robot, $\mathbf{t}_G^W \in \mathbb{R}^3$,$\mathbf{R}_G^W \in \mathbb{SO}(3)$ are the translation and rotation between the GNSS frame G and the global map frame W respectively, and $\mathbf{t}_W^I \in \mathbb{R}^3$,$\mathbf{R}_W^I \in \mathbb{SO}(3)$ are the translation and rotation between W and the current inertial frame of the robot I respectively. In addition, $\mathbf{p}_I \in \mathbb{R}^3$ is the position of the GNSS sensor in the inertial frame I of the robot, and is always fixed and can be calibrated with high precision. The value $\boldsymbol{\nu}_I \sim \mathcal{N}(\mathbf{0}, Q_{\mathrm{GNSS}}) \in \mathbb{R}^3$ models the uncertainty of the GNSS measurements, which is considered to follow a Gaussian noise model with zero mean and covariance Q_{GNSS}.

The residual given this measurement can be computed as $\mathbf{z}_G - \mathrm{h}(\mathbf{x}, \boldsymbol{\nu})$, being $\mathbf{z}_G \in \mathbb{R}^3$ the measured position in the GNSS frame. Next, the integration of GNSS in the *ikFoM* requires the derivation of two Jacobians as pointed out in (Xu et al., 2022; He et al., 2021). Assuming the robot state is fully represented by $\mathbf{x} = \{\mathbf{t}_W^I, \mathbf{R}_W^I\, \mathbf{t}_G^W, \mathbf{R}_G^W\}$, the Jacobians are derived as:

$$\mathbf{H} = \left. \frac{\partial \mathrm{h}(\mathbf{x} \boxplus \delta\mathbf{x}, \mathbf{0})}{\partial \delta\mathbf{x}} \right|_{\delta\mathbf{x}=\mathbf{0}} = \begin{bmatrix} \mathbf{R}_G^W & -\mathbf{R}_G^W \mathbf{R}_W^I \lfloor \mathbf{p}_I \rfloor & \mathbf{I}_3 & -\mathbf{R}_G^W \lfloor \mathbf{T}_W^I \mathbf{p}_I \rfloor \end{bmatrix} \quad (2)$$

$$\mathbf{D} = \left. \frac{\partial \mathrm{h}(\mathbf{x}, \boldsymbol{\nu})}{\partial \boldsymbol{\nu}} \right|_{\boldsymbol{\nu}=\mathbf{0}} = \mathbf{R}_G^W \mathbf{R}_W^I \quad (3)$$

The $\lfloor \cdot \rfloor$ operator represents the skew-symmetric transformation applied to a vector $\in \mathbb{R}^3$. The $\boxplus$ operator associates a certain perturbation defined in $\mathbb{R}^n$ to a perturbation of a point on a manifold trough a locally homeomorphic space (He et al., 2021). Using Jacobian $\mathbf{D}$, the covariance of the measurement model is projected into the reference frame G as $\bar{Q}_{\mathrm{GNSS}} = \mathbf{D} Q_{\mathrm{GNSS}} \mathbf{D}^T$, which is the value used in the *ikFoM*. Finally, the translation and rotation between the GNSS and the global frame have to be given an initial guess and an initial covariance. All of these values can be carefully calibrated except the yaw-axis rotation between them. Thus, we gave null confidence to that value, such that the initial angle to the north of the GNSS can be estimated by the *LiDAR-based mapping* module.

4. LiDAR-based powerline segmentation

Powerline inspection involves making accurate measurements of the distance between vegetation and powerlines, between vegetation and electrical towers, and additionally the vegetation density. Extracting these measurements requires segmenting powerlines, electrical towers, vegetation, and soil from the 3D map. The available information from the LiDAR includes the 3D (x, y, z) position of each point in the inertial coordinate system and the reflectivity (r) of the surface that was hit by the laser beam. This information is used to classify each point into four classes: *Powerline*, *Tower*, *Soil*, and *Vegetation*.

Reflectivity is a measure of the ability of a surface to reflect radiation. It depends on the material of the object that caused the reflection, the surface roughness and disposition, and the incidence angle. Hence, it is useful to distinguish between types of objects. Experimentally we observed that powerlines and towers offer reflectivity values significantly different to trees and soil. The adopted method classifies LiDAR points using a combination of the LIDAR reflectivity and the spatial distribution of the acquired points, (Valseca et al., 2022). First, the histogram of the reflectivity of the points is obtained. Then, LiDAR points are classified into two sets: *Metallic*, which includes the points corresponding to powerlines and towers; and *Organic*, which includes the points corresponding to vegetation and soil. We use an optimal threshold within the histogram for the classification which is calculated using the Gaussian Mixture Model method. Dual return points coming from canopy penetration are included in the *Organic* set, since they do not provide a reflectivity value but are virtually always representing either soil or vegetation. After this classification, a local spatial filter is applied to avoid outliers. Next, the points assigned to set *Metallic* are classified into classes *Powerline* and *Tower* with local Principal Component Analysis (PCA) using the fact that powerlines are (locally) distributed in one direction while the towers are not, and then a Mahalanobis distance-based region growing algorithm is used to generate clusters of points of type *Powerlines* and *Tower*. Finally, the points that were assigned to set *Organic* are clustered using region growing and then each cluster is classified using PCA into classes *Vegetation* and *Soil*.

Figure 4 shows a segmented LiDAR-based map obtained in one experiment performed in ATLAS, a Test Flight Centre located at Villacarrillo (Jaen). The points are shown in different colors depending on its class: *Powerlines* (green), *Towers* (red), *Vegetation* (yellow), and *Soil* (Blue).

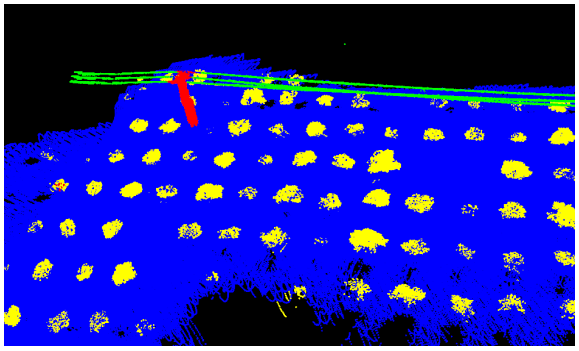

Figure 4: Segmented map represented with different color for each class: *Powerlines* (green), *Towers* (red), *Vegetation* (yellow), and *Soil* (blue).

5. Experimental validation

The proposed aerial robotic system was validated in sets of powerline inspection flights performed in different scenarios with varied conditions, including different types of vegetation and terrain. It was first tested in preliminary experiments performed in: i) School of Engineering of Seville (ETSI, Seville, Spain), ii) Burguillos (Seville, Spain), and iii) Alcala de Guadaira (Seville, Spain). In all the scenarios, the *LR-M* robot followed the powerline and mapped the surrounding environment, except in the ETSI scenario, where an urban area near the School of Engineering of the University of Sevilla was mapped. In the ETSI experiments the accuracy of the maps provided by *LR-M* was compared versus ground truth maps generated by a Leica Total Station. This analysis could not be done in the other scenarios due to their significantly larger size, terrain

height differences, and vegetation occlusions. Figure 5 shows the distribution of the absolute mapping error obtained. The mean absolute mapping error is lower than 1 cm, with a RMSE error lower than 4 cm, hence validating the accuracy of the proposed system. It should be noticed that the Leica Total Station took more than one hour to obtain the map in this scenario, whereas *LR-M* built it online in a flight of less than 5 min.

The proposed robotic system was then validated in experiments conducted in the ATLAS Flight Test Center at Villacarrillo (Jaen), see Figure 6-top. ATLAS includes several kilometers of powerlines of different voltages within its 35x31 km^2 of segregated aerial space. The experiments consisted in using *LR-M* to build a map in a long-range powerline inspection mission. The robot *LR-M* was commanded to autonomously follow a Beyond Visual Line of Sight (BVLS) trajectory specified with a set of 13 waypoints in a mission covering more than 3.5 km (1.8 km go and back), see Figure 6-bottom. The robot average speed was set to 5 m/s.

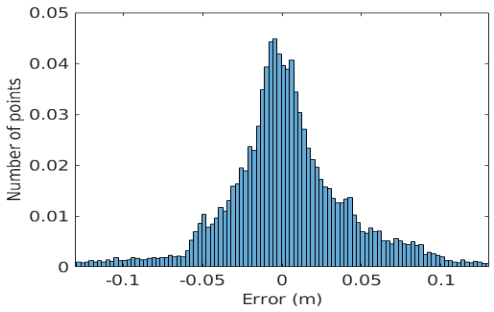

Figure 5: Distribution of the absolute error between the map computed by *LR-M* and ground truth maps generated by a Leica Total Station in the ETSI scenario.

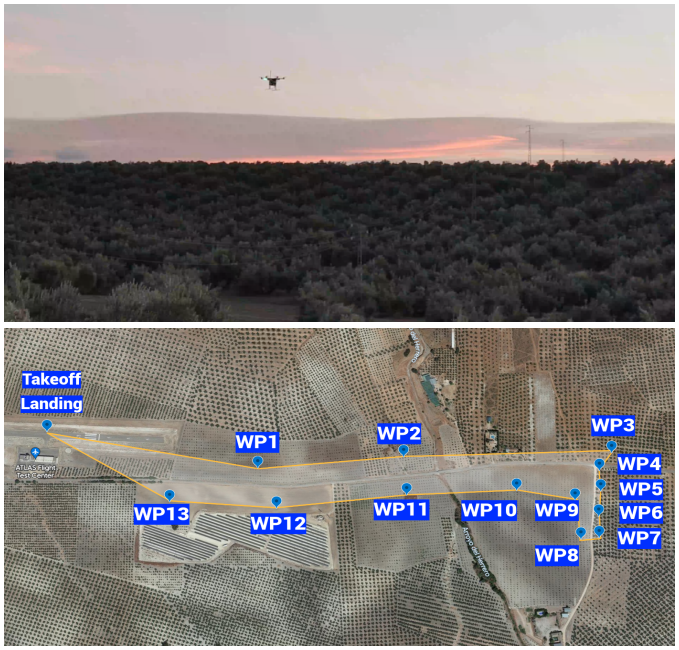

Figure 6: Top) Picture taken in powerline mapping experiments in ATLAS. Bottom) Trajectory (3.5 km) followed by *LR-M* in the desribed experiment.

The robot navigated the trajectory fully autonomously using the GNSS-based navigation modules shown in Figure 1. The measurements and images from the different sensors were logged. Simultaneously, they were used to online build the map as described in Section 3. Along the flights, the online mapping system was able to run onboard at 10Hz, the LiDAR refresh rate, and memory consumption was always lower than the 16GB available at the Jetson Xavier NX. A detail of the 3D map computed ontime and on board is shown in Figure 7. The map is colored with the reflectivity value of each point. After the flight, the LiDAR-based segmentation method described in Section 4 was executed to classify the map points. The resulting segmented map obtained in the experiment of $> 3.5km$ long is shown in Figure 8.

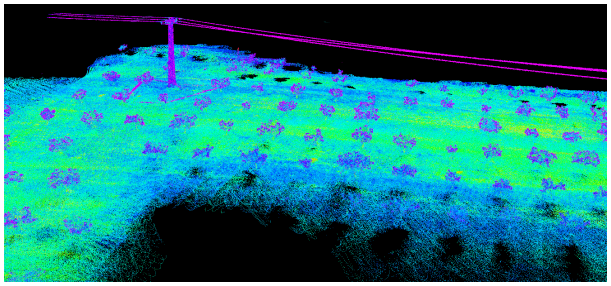

Figure 7: Detailed map of the target powerline inspected in ATLAS.

6. Conclusions

A wide variety of research prototypes and commercial systems based on different types of vehicles have been developed for powerline inspection using platforms such as unmanned helicopters, fixed-wing vehicles, VTOLs, and also multicopters. However, most existing systems and schemes adopt inspection procedures that consist of two stages. First, the robot collects data of the environment. Second, the data is post-processed offline days after data collection and often in the laboratory, to obtain the map and actually perform the powerline inspection. This procedure prevents operators from being sure that the collected data are actually of suitable resolution and quality, hence potentially requiring repeating the data collection flight flights weeks after, causing delays, costs, and operational problems.

This paper presented a fully autonomous aerial robot for online and on board building of accurate 3D maps for long-range powerline inspection. The robot is equipped with a 3D LiDAR, an RGB camera, an onboard computer, a GPS receiver, and an IMU, and includes a fully onboard architecture with modules for autonomous navigation and online LiDAR-based mapping through a method inspired in *FAST-LIO2* but modified to also integrate GNSS. The robotic system also includes a module that processes the built 3D map and detects (using reflectivity and geometrical criteria) objects of interest in powerline inspection scenarios. The robot has been widely validated in experiments performed in different powerline scenarios, providing a mean absolute mapping error lower than 1 cm, and with an RMSE lower than 4cm.

The presented system provides a reliable, immediately-available map during flight time, opening wide areas of future research and development. The system can be integrated with schemes that can leverage the available 3D map for performing

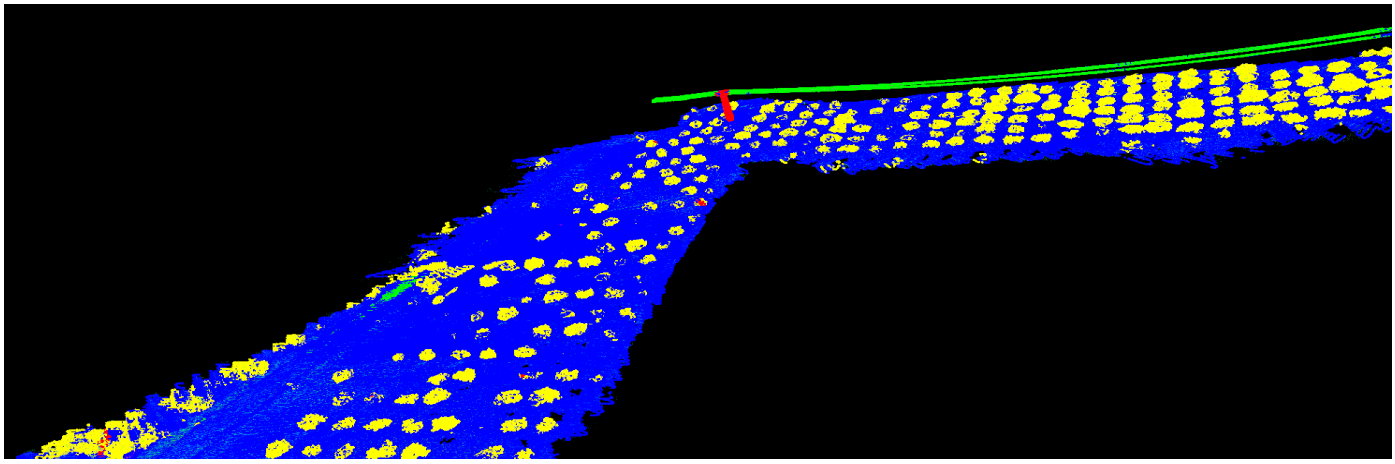

Figure 8: Segmented map resulting from long range powerline inspection in ATLAS scenario.

automated improvements and corrections to the robot's trajectory to enhance inspection. The inclusion of texture information coming from RGB or other cameras (hyper-spectral, polarimetric) can highly benefit the proposed map building and segmentation systems. Given the modularity of the presented approach, these new areas of research could be explored without requiring significant changes in the software architecture.

Acknowledgements

This work was supported by the European Union's Horizon 2020 Programme under grant agreement No. 871479 (AERIAL-CORE), by the Spanish Projects ROBMIND (Ref. PDC2021-121524-I00) from the Programa Estatal de I+D+i, RIME (Ref. AT21-00061) from the Regional Goverment of Andalucia, and by the Spanish Ministerio de Universidades FPU Program (FPU17/0632).

References

Bhola, R., Krishna, N. H., Ramesh, K., Senthilnath, J., Anand, G., 2018. Detection of the power lines in uav remote sensed images using spectral-spatial methods. Journal of environmental management 206, 1233–1242.

Bian, J., Hui, X., Zhao, X., Tan, M., 2018. A novel monocular-based navigation approach for uav autonomous transmission-line inspection. In: 2018 IEEE/RSJ IROS. pp. 1–7.

Deng, C., Wang, S., Huang, Z., Tan, Z., Liu, J., 2014. Unmanned aerial vehicles for power line inspection: A cooperative way in platforms and communications. J. Commun. 9 (9), 687–692.

He, D., Xu, W., Zhang, F., 2021. Kalman filters on differentiable manifolds. arXiv preprint arXiv:2102.03804.

Jenssen, R., Roverso, D., et al., 2019. Intelligent monitoring and inspection of power line components powered by uavs and deep learning. IEEE Power and energy technology systems journal 6 (1), 11–21.

Jwa, Y., Sohn, G., Kim, H., 2009. Automatic 3d powerline reconstruction using airborne lidar data. Int. Arch. Photogramm. Remote Sens 38 (Part 3), W8.

Kitchen, R., Bierwolf, N., Harbertson, S., Platt, B., Owen, D., Griessmann, K., Minor, M. A., 2020. Design and evaluation of a perching hexacopter drone for energy harvesting from power lines. In: 2020 IEEE/RSJ IROS. pp. 1192–1198.

Li, H., Wang, B., Liu, L., Tian, G., Zheng, T., Zhang, J., 2013. The design and application of smartcopter: An unmanned helicopter based robot for transmission line inspection. In: 2013 Chinese Automat. Congress. pp. 697–702.

Li, K., Li, M., Hanebeck, U. D., 2021. Towards high-performance solid-state-lidar-inertial odometry and mapping. IEEE Robotics and Automation Letters 6 (3), 5167–5174.

Lin, J., Zhang, F., 2020. Loam livox: A fast, robust, high-precision lidar odometry and mapping package for lidars of small fov. In: 2020 IEEE ICRA. pp. 3126–3131.

Liu, C., Wang, L., Liu, C., 2009. Mission planning of the flying robot for powerline inspection. Progress in Natural Science 19 (10), 1357–1363.

Liu, Y., Shi, J., Liu, Z., Huang, J., Zhou, T., 2019. Two-layer routing for high-voltage powerline inspection by cooperated ground vehicle and drone. Energies 12 (7), 1385.

Martinez, C., Sampedro, C., Chauhan, A., Collumeau, J. F., Campoy, P., 2018. The power line inspection software (polis): A versatile system for automating power line inspection. Engineering Applications of Artificial Intelligence 71, 293–314.

Paneque, J., Martínez-de Dios, J., Ollero, A., 2019. Multi-sensor 6-dof localization for aerial robots in complex gnss-denied environments. In: 2019 IEEE/RSJ IROS. pp. 1978–1984.

Paneque, J. L., Dios, J. R. M.-d., Ollero, A., Hanover, D., Sun, S., Romero, A., Scaramuzza, D., 2022. Perception-aware perching on powerlines with multirotors. IEEE Robotics and Automation Letters 7 (2), 3077–3084.

Perez-Grau, F. J., Martinez-de Dios, J. R., Paneque, J. L., Acevedo, J. J., Torres-González, A., Viguria, A., Astorga, J. R., Ollero, A., 2021. Introducing autonomous aerial robots in industrial manufacturing. Journal of Manufacturing Systems 60, 312–324.

Real, F., Torres-González, A., Ramón-Soria, P., Capitán, J., Ollero, A., 2020. Unmanned aerial vehicle abstraction layer: An abstraction layer to operate unmanned aerial vehicles. Int. J. of Advanced Robotic Systems 17 (4).

SDK, L., 2020. Livox-mapping. `https://https://github.com/Livox-SDK/livox_mapping`.

Takaya, K., Ohta, H., Kroumov, V., Shibayama, K., Nakamura, M., 2019. Development of uav system for autonomous power line inspection. In: 23rd Int. Conf. on System Theory, Control and Computing. pp. 762–767.

Valseca, V., Paneque, J., Martínez-de Dios, J. R., Ollero, A., 2022. Real-time lidar-based semantic mapping for powerline inspection. In: 2022 Int. Conf. on Unmanned Aircraft Systems.

Wang, B., Han, L., Zhang, H., Wang, Q., Li, B., 2009. A flying robotic system for power line corridor inspection. In: IEEE Int. Conf. on Robotics and Biomimetics. pp. 2468–2473.

Wang, M., 2021. Inspection technology of remote transmission towers based on a vertical take-off and landing fixed-wing uav. In: Journal of Physics: Conference Series. Vol. 1865. IOP Publishing, p. 022076.

Xu, W., Cai, Y., He, D., Lin, J., Zhang, F., 2022. Fast-lio2: Fast direct lidar-inertial odometry. IEEE Transactions on Robotics, 1–21.

Yi, W., Liming, C., Lingyu, K., Jie, Z., Miao, W., 2017. Research on application mode of large fixed-wing uav system on overhead transmission line. In: IEEE Int. Conf. on Unmanned Systems. pp. 88–91.

Zhang, W., Wu, X., Zhang, G., Ke, L., Chen, L., Chen, X., Yang, H., Qiao, X., Zhou, Y., 2016. The application research of uav-based lidar system for power line inspection. In: 2nd Int. Conf. on Computer Engineering, Information Science & Application Technology. pp. 989–993.

Zhen, L., Li, M., Laporte, G., Wang, W., 2019. A vehicle routing problem arising in unmanned aerial monitoring. Computers & Operations Research 105, 1–11.